Engineering Fracture Mechanics Vol. 34, No. 4, pp. 785–802, 1989
Printed in Great Britain.

0013-7944/89 $3.00 + 0.00
Pergamon Press plc.

STATISTICAL BEHAVIOUR OF FATIGUE CRACK GROWTH FOR HY-80 STEEL PLATE AND ITS WELDMENTS UNDER CATHODIC PROTECTION IN SEAWATER AND IN AIR

J. R. MATTHEWS,† T. BETANCOURT‡ and M. ROBICHEAU‡

†Defence Research Establishment (Atlantic), P.O. Box 1012, Dartmouth, N.S. B2Y 3Z7 Canada
‡Nova Scotia Research Foundation Corporation, P.O. Box 790, Dartmouth, N.S. B2Y 3Z7, Canada

Abstract—This paper deals with fatigue crack growth data for various weldments of HY-80 steel plate in seawater and a statistical method for using this data in life predictions and deviations from mean life estimates. Typical results of crack growth behaviour with crack length and examples of the effect of averaging increment on variability of crack growth data are given. The standard deviation for incremental crack growth rates are determined. Use of the data in the calculation of confidence limits in life cycle determination are discussed. The A and N data, from which crack growth data were obtained, were generated on HY-80 base plate and HY-80 weld containing compact tension specimens. They were fatigue-tested either in air at 23°C or in seawater at 23°C. Specimens tested in seawater were also galvanically protected with zinc electrodes. Fatigue loading was at constant ΔK and $R = 0.1$ or 0.5. Frequency of loading was 0.3 Hz.

1. INTRODUCTION

HISTORICALLY, the objective in fatigue crack growth testing has been aimed at estimating the mean trend in da/dN for different conditions and accounting for observed variability in a somewhat subjective manner [1]. This process recognizes that the scatter can result from both material properties as well as data recording, reduction and analysis methods. Isolating the proportion of the total variation that is due to inherent material properties and using this component to predict variation in fatigue lives has been a difficult research objective.

In this paper, two observations about the fatigue process and its analysis have led to a Monte Carlo style approach to provide a statistical treatment of fatigue life prediction for actual da/dN data. The first observation is that the averaging increment [2] used to analyse the data must be the same as the increment used in a statistial life prediction. The second observation is that the majority of variability can be linked to the deviation of the crack from normal. When the crack proceeds straight ahead, it moves fastest and when it deviates up or down (right or left) from the straight ahead crack line, it slows down. As it returns to the straight ahead direction, it speeds up again. This produces a spatial period in da/dN vs a data which matches the actual period of up and down deviation from the straight ahead crack. Furthermore, the averaging increment absorbs the variation in measurement errors as it is taken longer and longer. At the lowest level of data recording (say 0.25 mm) the variation in measurement error is the same order of magnitude as the measurement but as the increment is taken longer and longer, this error effect is reduced.

Accordingly, having physically witnessed the major cause of variation (crack deviation) and noting that measurement errors and analysis consistency are reduced by taking a fixed increment of crack extension (around 0.51 mm), the Monte Carlo approach to life prediction was laid out.

In this paper, a Monte Carlo technique for prediction of crack growth lives is given for a standardized fatigue crack growth data generating approach and fatigue crack growth data for various weldments of HY-80 to be used with this approach are presented.

2. THE MODEL

It is assured that the actual scatter in the generated data is typical of the scatter in growth rate in an actual component or structure. In the first place, this is not all that unrealistic because the specimen itself is a component. The important link between the analysis and the data acquisition

is the crack increment chosen. This does not affect the mean life but it does affect predicted deviation in mean life and scatter in test results. Accordingly, using a constant ΔC in data reduction and analysis, forces a realistic correspondence in data scatter and prediction in deviation in mean life. In the second place, there is a correspondence between the crack growth in one set of cycles in a test and in the set which preceded it and followed it. This linking is due to the observed phenomenon of crack deviation controlling scatter in growth rate and the fact that the change in growth rate is quite gradual, almost periodic in some cases. Accordingly, it is reasonable to use data generated in a non-independent manner to allow prediction of growth in a structure in an independent analysis because the crack growth in the structure in a particular location will be influenced by the growth rate immediately before that location and it will affect that rate to follow.

The ultimate calculated values are mean life and estimated deviation in mean life. The non-independent data reduction scheme to follow will simply require growth rates averaged over crack increments equal to those used in the calculation and a knowledge of the distribution of the scatter in growth rate for each K_{max}, R ratio, frequency and environmental condition of interest.

3. DATA REDUCTION

The non-independent data reduction scheme is as follows:

(1) The number of cycles for the crack to grow each 0.25 mm increment (at fixed ΔK) was recorded. Note that the absolute value of crack length would not be predicted well but the number of cycles between successive 0.25 mm increments would be predicted quite well. It was determined that the number of cycles would be estimated with an accuracy of $\pm 30\%$ at this small increment. However, this error will be greatly reduced by larger increments as used later in the data reduction scheme.

(2) This produced 200 delta n increments (say, $n1$, $n2$, ... $n200$) since the cracks were grown from approximately 22.8 to 27.9 mm.

(3) da/dN values were then calculated in an overlapping non-independent manner for different ΔC increments. For example, if ΔC increment were chosen at 0.25 mm, then ten of the data increments would be combined. The number of cycles in the first increment would be $n1 + \ldots + n10$, in the second increment, $n2 + \ldots + n11$, etc. That is, there would be about 190 da/dN values since 10 recorded values would be needed at the end of the sequence. Any two consecutive increments would have nine values of n in common. This is a non-independent data reduction technique.

(4) In a similar manner, if the crack growth increment was selected to be 2.5 mm, each increment would require the sum of 100 of the recorded increments and there would be about 100 da/dN values and any two consecutive increments would have 99 values of n in common. The data thus generated would be highly correlated and the high correlation would have to be taken into consideration in the analysis plan of the Monte Carlo scheme if the high ΔC were used. Basically, at low ΔCs, the experimental error dominates, while at high ΔCs, the high correlation of the data reduction dominates. It remains to choose an intermediate ΔC that is not affected seriously by both when the analysis is carried out. Ultimately, an enormous bank of independent, uncorrelated da/dN data would be preferable but for the purpose of our work and analysis, it is not expedient.

4. EXAMPLE OF DATA REDUCTIONS

Table 1 is an example of data reduction for data generated with $\Delta C = 1.27$ mm, K and R constant.

The data is then plotted directly on a da/dN vs ΔK standard plot with the increment for the correlated data reduction clearly indicated (i.e. $\Delta C = 1.27$ mm, see Fig. 1).

When considerable data has been generated for a given condition, ΔK, R, increment, etc., at a fixed value of ΔC, it remains to determine the distribution of the data. A plot of typical data is shown in Fig. 2. This indicates that a quasi-normal distribution of crack growth exists about the mean growth rate. In physical terms, the crack spends more time off the normal straight ahead

Table 1. Data Reduction

N(cycles)	a (mm)	da/dN (μm/cycle) and a (mm)
0	22.8595	$\frac{\Delta a}{\Delta n_1} = \frac{24.1325 - 22.8595}{2330-0} = .5487$
61	22.8867	$a_1 = (22.86 + 24.13)/2 = 23.49$
112	22.9113	$\frac{\Delta a}{\Delta n_2} = \frac{24.1562 - 22.8867}{2372-61} = .5493$
2320	24.1325	$a_2 = (22.89 + 24.16)/2 = 23.52$
2372	24.1562	$\frac{\Delta a}{\Delta n_3} = \frac{24.1849 - 22.9113}{2402-112} = .5562$
2402	24.1849	$a_3 = (22.91 + 24.18)/2 = 23.55$

direction than on it. This distribution is the final piece needed for the analysis technique. In the next part of this paper, the analysis technique will be described while in the later part of this paper, specific data for welded HY-80 material will be given.

5. ANALYSIS TECHNIQUE

To determine mean life and an estimated deviation from the mean life for a particular amount of crack growth in a given component, one can use the following Monte Carlo scheme.

(1) Define the range of cracking of interest in the component, initial crack size, c_i, to final crack size, c_f (say, 22.5–25 mm).
(2) Divide the crack into increments of crack length, ΔC, equal to the increment used in the data reduction for generating data for the material and conditions of interest (i.e. R and environment) (say, 0.50 mm, for example).
(3) Using an exact solution or finite element or boundary element analysis, calculate the maximum stress intensity, K_1, that will exist at the mid-point of each increment.
(4) Using a random number generator tailored to the form of the distribution of the data, randomly, values of da/dN for each K value and then calculate

$$\Delta N_i = \frac{\Delta C}{da/dN_{\text{random}}}.$$

(5) Add the values of ΔN so determined to calculate a potential life for the given crack extension ΔN_T.
(6) Repeat the above 20 times and then calculated a mean life and standard deviation

$$\bar{\Delta N} = \sum_{i=1}^{20} \Delta N_{Ti}/20$$

and

$$\sigma_N = \sqrt{\sum_{i=1}^{20} (\Delta N_i - \Delta N)^2/(20-1)}.$$

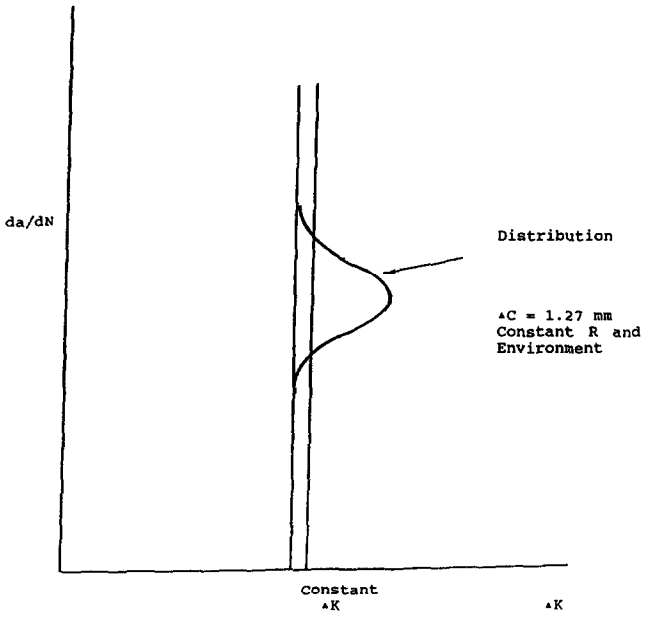

Fig. 1. Method of recording the generated da/dN data.

(7) Subtracting 3σ from $\bar{\Delta}N$ gives a lower value for expected crack growth cycles that can be used with great confidence in any inspection dominant plan for safety of a structure. A tabular display of this scheme is shown in Table 2.

In the balance of this paper specific data will be presented for HY-80 steel plate weldments under cathodic protection in seawater and in air that can be used in this type of analysis.

6. EXPERIMENTAL

In this work, all extraneous factors, such as experimental conditions and data processing, affecting the variability of da/dN were strictly controlled[3, 4]. The crack length and number of cycles were both determined repeatedly at each ΔK. Data acquisition was made between 22.86 and

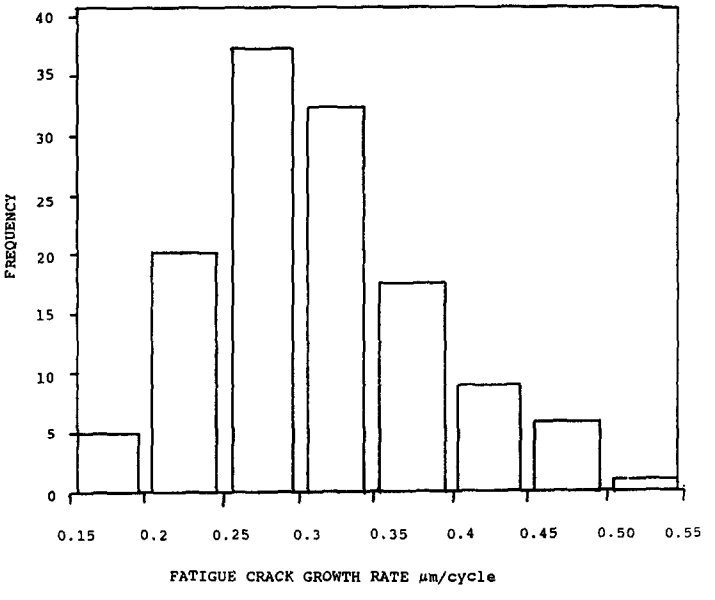

Fig. 2. Typical histogram showing distribution of fatigue crack growth rate frequency for fixed ΔK, R and environment.

Table 2. Tabular display of Monte Carlo scheme

	K	Step 1	Step 2	Step 3	...	Step 20
C1–C2	$K1$	$\Delta N1$	$\Delta N4$	$\Delta N11$	...	$\Delta N96$
C2–C3	$K2$	$\Delta N2$	$\Delta N7$	$\Delta N12$	...	$\Delta N97$
C3–C4	$K3$	$\Delta N3$	$\Delta N4$	$\Delta N13$	...	$\Delta N98$
C4–C5	$K4$	$\Delta N4$	$\Delta N9$	$\Delta N14$	...	$\Delta N99$
C5–C6	$K5$	$\Delta N5$	$\Delta N10$	...	...	$\Delta N100$
		ΔNT_1	ΔNT_2	ΔNT_3	...	ΔNT_{20}

Note. $\bar{\Delta N} = \sum_{i=1}^{20} \Delta N_{Ti}/20$; and $\sigma_N = \sqrt{\sum_{i=1}^{20} (\Delta N_i - \Delta N)^2/(20-1)}$.

278.94 mm by recording the number of applied load cycles each time the crack grew ~0.025 mm as indicated by the crack opening displacement COD clip gauge method. As mentioned in the Introduction, the absolute value of crack length had an error between 1 and 3%, depending on the system used (as verified by breaking samples open at various crack lengths and measuring directly on the specimen). Also, there is an instability in the crack measurement at such low levels which affects the cycles involved in a particular amount of crack extension prediction as well. This can be as much as a 30% variation on 0.025 mm measurements. This error diminishes as Δa increases.

The ΔK of each experiment was controlled to within 0.1%. All specimens during the data acquisition were fatigued in air or submerged in seawater and galvanically protected with two zinc electrodes; one electrode on each side of the test specimen (as illustrated in Fig. 3). The flow of seawater through the cell was maintained at 2.5 l/h.

The basic procedure for determining crack length from measurements of COD in CT specimens are well-documented[5]. The COD calibration expressions developed by Roberts[6] and slightly modified by Jablonski and Lee[7] were used throughout this work.

The corrosion fatigue crack propagation rate testing was performed on a computer controlled 1.02 kN electrohydraulic closed-loop materials testing system. All tests were done at an ambient temperature of 23°C ± 1°C using tension–tension loading and a sinusoidal waveform. A cyclic frequency of 0.3 Hz and load ratios $R = P_{min}/P_{max}$ of 0.1 and 0.5 were used. This frequency was primarily chosen for convenience. The loading frequency of the structures of interest to the authors is five orders of magnitude slower.

7. SPECIMENS

All specimens including those containing welds were made from rolled low alloy HY-80 plate steel. The test specimens were compact type (CT) with thickness ranging from 21.59 to 25.4 mm. The crack orientation in weldments was as illustrated in Fig. 4.

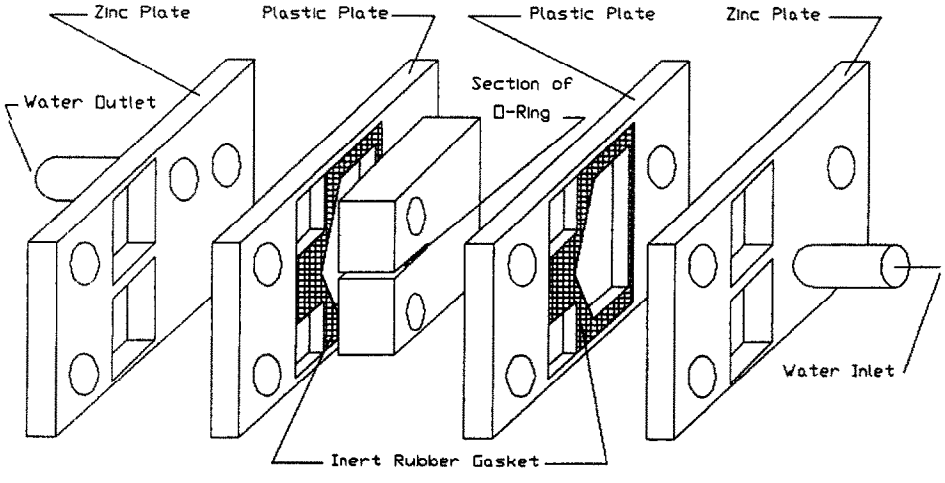

Fig. 3. Main components of the corrosion cell.

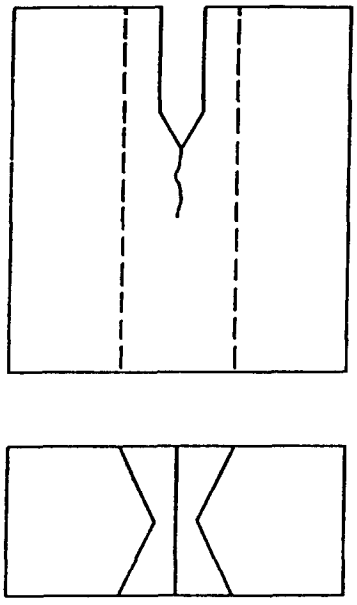

Fig. 4. Orientation of cracks in welded plate specimens.

Table 3 summarizes the materials studied in this work. A large number of samples were taken from each plate identified.

The first four plates studied contained weldments that were produced using pulsed gas metal arc welding, GMAW, techniques[8]. The Generac is a Japanese MITSUBISHI welding unit and the Espel is a Welding Institute of Canada development. The generac, like the original AWP UK synergic pulsed GMAW system, uses wire feed and voltage feedback control while the frequency modulated Espel unit uses only voltage feedback control. The 4th, 5th, 6th, and 9th plates contained weldments that were prepared at the Ship Repair Unit Atlantic of DND in Halifax under conditions typical of submarine pressure hull welding. The 7th and 8th plates contained weldments that were produced with the patented Transfer Ionized Molten Energy (TIME) process[9]. This is a standard GMAW welding process enhanced by a special gas (25–35% He, 6.7–8.5% CO_2 and 0.3–0.8% O_2 bal Ar). These weldments were made with AWS 70S1 and 100S1 wires with a narrow gap (NG) joint configuration. The final set of samples came from as-received HY-80 base plate with notches oriented in the transverse and longitudinal directions.

8. RESULTS

The crack propagation data are in Table 4. This is a summary table and represents data from experiments carried out at $R = 0.1$ and $R = 0.5$. It contains mean data da/dN and standard

Table 3.

Plate	Description
4	4 (260) MIG Generac Flat
5	5 (261) MIG Espel Vertical
8	8 (264) MIG Generac Vertical
10	10 (266) MIG Espel Flat
5/6	5/6 SMAW/E11018M
7/8	7/8 SMAW/E9018M
9/10	9/10 SMAW/E7018
1	NG/70S1 Time 1
3	NG/100S1 Time 2
90E1	90E1 SMAW/E9018M
90G1	90G1 Base Plate/HY-80 (T)
90F1	90F1 Base Plate/HY-80 (L)

(T) is the orientation of crack perpendicular to the direction of rolling.

(L) is the orientation of crack in rolling direction.

Table 4. Incremental crack growth data

Specimen	Plate	Environment	ΔK, MPa$\sqrt{m}$	R	Crack propagation data Mean, da/dN μm/cycle	Averaging increment, ΔC mm	Standard deviation μm/cycle
W9/10-1	9/10SMAW/E7018	SW + CP	29.7	0.1	0.053	0.25	0.019
						0.51	0.012
						1.27	0.009
W10-2	10 (266) MIG Espel Flat	SW + CP	29.70	0.1	0.119	0.25	0.073
						0.51	0.024
						1.27	0.018
T2	Base Plate/HY-80 (T)	SW + CP	29.7	0.1	0.181	0.25	0.011
						0.51	0.004
						1.27	0.001
F1	NG/70S1 TIME 1	SW + CP	29.7	0.1	0.211	0.25	0.100
						0.51	0.046
						1.27	0.023
D1	NG/100S1 TIME 2	SW + CP	29.7	0.1	0.108	0.25	0.055
						0.51	0.026
						1.27	0.007
13	Base Plate/HY-80 (T)	Air	49.5	0.1	0.541	0.51	0.013
15	Base Plate/HY-80 (T)	Air	49.5	0.1	0.538	0.51	0.015
6	Base Plate/HY-80 (T)	Air	49.5	0.1	0.537	0.51	0.012
14	Base Plate/HY-80 (T)	Air	49.5	0.1	0.538	0.51	0.015
4	Base Plate/HY-80 (L)	Air	49.5	0.1	0.660	0.51	0.016
9	Base Plate/HY-80 (L)	Air	49.5	0.1	0.660	0.51	0.019
10	Base Plate/HY-80 (L)	Air	49.5	0.1	0.656	0.51	0.191
W4-5	4 (260) MIG Generac Flat	SW + CP	22.0	0.5	0.085	1.27	0.004
						0.51	0.011
						0.25	0.022
						0.05	0.307
W44-1	4 (260 MIG Generac Flat	SW + CP	22.0	0.5	0.056	0.51	0.011
W7/8-1	7/8 SMAW/E9018M	SW + CP	22.0	0.5	0.131	1.27	0.005
						0.51	0.011
						0.25	0.029
						0.05	0.112
90G1-2	90G1 Base Plate/HY-80 (T)	SW + CP	22.0	0.5	0.168	1.27	0.004
						0.51	0.007
						0.25	0.009
						0.05	0.024
90G2-1	90G2 Base Plate/HY-80 (T)	SW + CP	22.0	0.5	0.238	0.51	0.002
W10-3	10 (266) MIG Espel Flat	SW + CP	22.0	0.5	0.088	0.51	0.022
W10-41	10 (266) MIG Espel Flat	SW + CP	22.0	0.5	0.136	0.51	0.006
W5/6-22	5/6 SMAW/E11018M	SW + CP	22.0	0.5	0.120	0.51	0.022
W7/8-22	7/8 SMAW/E90118M	SW + CP	22.0	0.5	0.130	0.51	0.026
W9/10-22	9/10 SMAW/E7018	SW + CP	22.0	0.05	0.270	0.51	0.003
W9/10-32	9/10 SMA/E7018	SW + CP	22.0	0.5	0.102	0.51	0.020
W90E-1	90E1 SMAW/E9018M	SW + CP	22.0	0.5	0.204	0.51	0.036
W5-1	5 (261) MIG Espel Vertical	SW + CP	19.8	0.5	0.220	0.51	0.002
W5-2	5 (261) MIG Espel Vertical	SW + CP	24.7	0.5	0.240	0.51	0.007
W8-1	8 (264) MIG Generac Vertical	SW + CP	19.8	0.5	0.028	0.51	0.802
W8-2	8 (264) MIG Generac Vertical	SW + CP	24.7	0.5	0.220	0.51	0.010
90G1-1	90G1 Base Plate/HY-80 (T)	SW + CP	19.2	0.5	0.116	0.51	0.002
90G2-2	90G2 Base Plate/HY-80 (T)	SW + CP	24.7	0.5	0.281	0.51	0.003
90E2-1	90E2 SMAW/E9018M	SW + CP	24.7	0.5	0.292	0.51	0.017
90E2-2	90E2 SMAW/E9018M	SW + CP	27.5	0.5	0.356	0.51	0.012
W42-2	4 (260) MIG Generac Flat	SW + CP	24.7	0.5	0.189	0.51	0.017
W42-1	4 (260) MIG Generac Flat	SW + CP	27.5	0.5	0.249	0.51	0.020

deviations. The table provides information about relative resistance in various materials to crack propagation. The crack rates at $R = 0.5$ appear to be generally higher than those obtained at $R = 0.1$. Also, the SMAW welds have somewhat lower resistance to corrosion fatigue at $R = 0.5$ than do the GMAW welds. From this table, it can be further concluded that welds have better resistance to crack propagation than the base plate. Crack growth rates were determined on the crack span ranging from 22.86 to 27.94 mm, and represent the mean crack rates. The variability

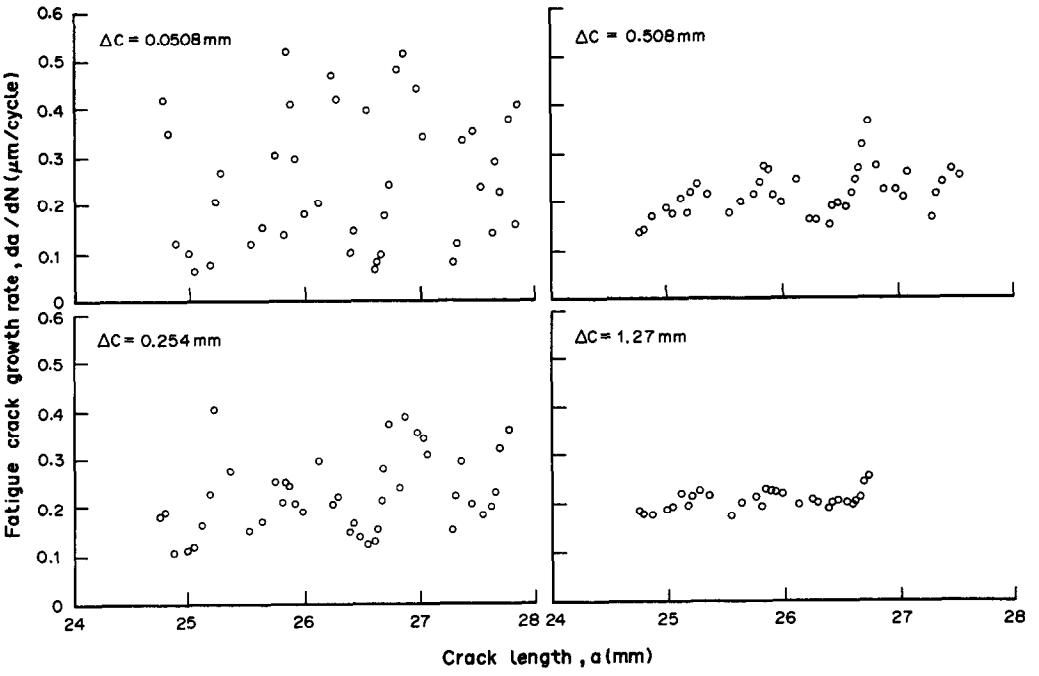

Fig. 5. Variability in da/dN with crack length a, in 90E1 SMAW/E9018M Weldment. Mean crack rate 0.194 microns/cycle. $\Delta K = 22$ MPa $\sqrt{m}$, $R = 0.5$.

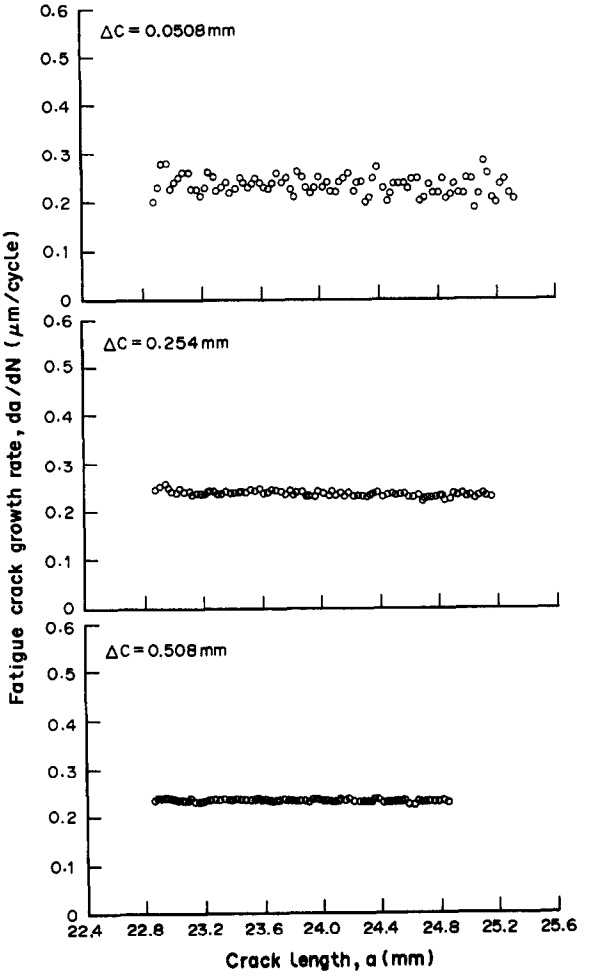

Fig. 6. Variability of da/dN with crack length a, in HY-80 base plate. Mean crack rate 0.204 microns/cycle. $\Delta K = 22$ MPa $\sqrt{m}$, $R = 0.5$.

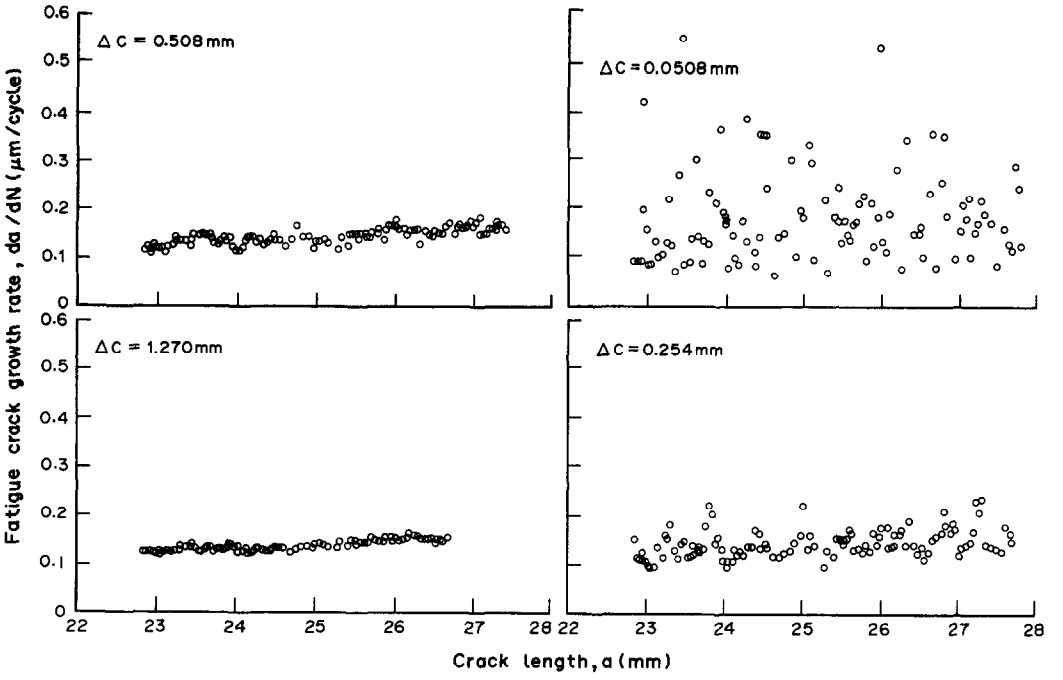

Fig. 7. Variability of da/dN with crack length a, in 7/8 SMAW/E9018 weldment. Mean crack rate 0.125 microns/cycle. $\Delta K = 22\,\text{MPa}\sqrt{m}$, $R \simeq 0.5$.

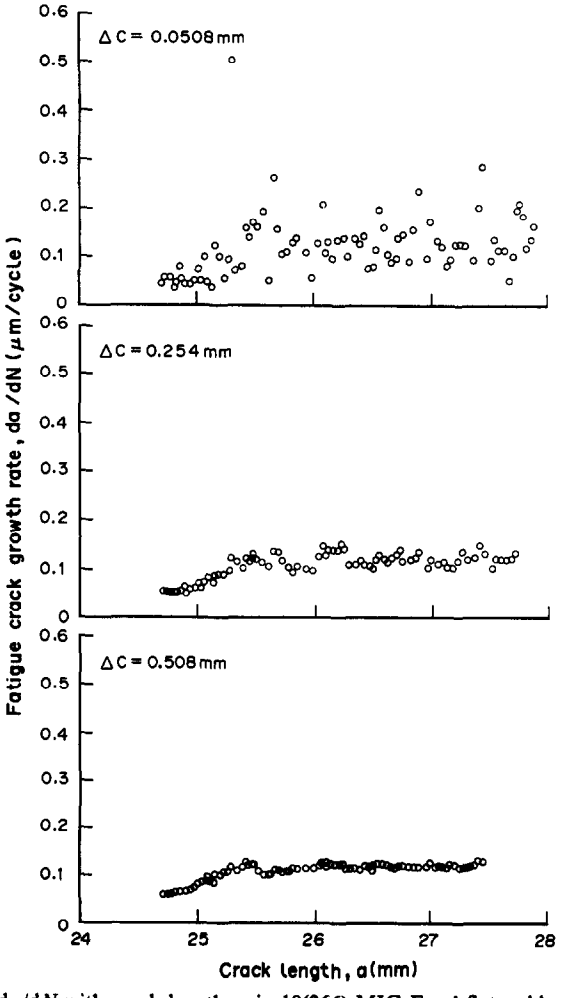

Fig. 8. Variability in da/dN with crack length a, in 10(266) MIG Espel flat weldment. Mean crack rate 0.101 microns/cycle. $\Delta K = 22\,\text{MPa}\sqrt{m}$, $R = 0.5$.

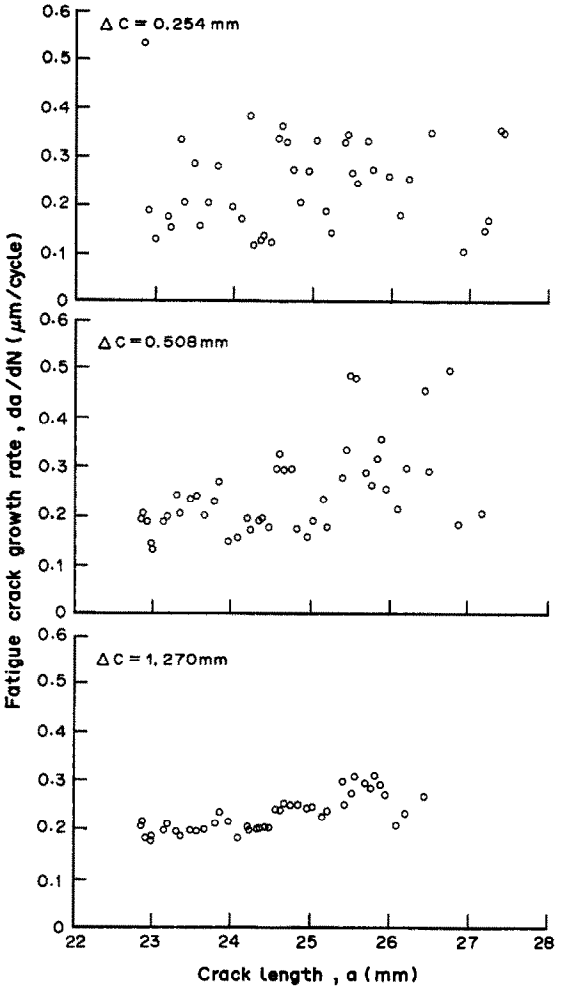

Fig. 9. Variability in da/dN with crack length a, in 100 S1(T2) narrow gap weldment. Mean crack rate 0.189 microns/cycle. $\Delta K = 29.7$ MPa $\sqrt{m}$, $R = 0.1$.

of crack growth rates is easily seen on plots of actual incremental crack growth data vs actual crack length shown in Figs 5–10. There are 3–4 graphs in each of these figures, representing data from a particular material, averaged over different crack increments. Figure 6, for example, shows crack growth behaviour through a 25 mm-thick CT base plate specimen, in which the crack orientation was perpendicular to the plate rolling direction. The individual rates, average over 0.05, 0.25 and 0.51 mm increments, are scattered around a mean rate and are close to normally distributed as in Fig. 2. On some plots, as the crack progresses through the specimen, the da/dN data shows spacial periodic behaviour corresponding to the crack deviation from normal. That is, when the crack is moving straight ahead, it advances the fastest, but as it branches in direction up and then below the normal straight ahead path, the spacial period is the same as the physical one.

Sample plots of crack growth data vs a for weldments indicate a much larger variability in crack growth rate than was seen in the base plate data. This increased variability in crack growth rate from weldments appears to have resulted from the microstructural heterogeneity of the welds and a corresponding increase in deviation from the horizontal crack plane. The base plate microsructure was fine-grained, while that of the welds through which these cracks grew was very coarse-grained. The coarsest was the structure of the GMAW weldments. The micrographs in Figs 11–13 show the typical structures in the base plate and weldments.

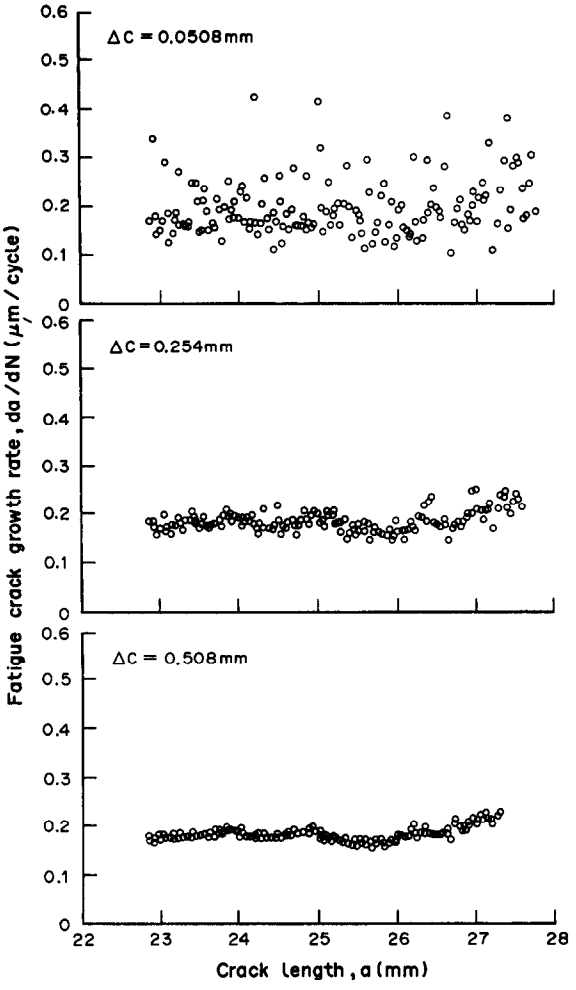

Fig. 10. Variability in da/dN with crack length a, in HY-80 base plate. Mean crack rate 0.193 microns/cycle. $\Delta K = 29.7$ MPa $\sqrt{m}$, $R = 0.1$.

9. DISCUSSION

For the data presented, the incremental crack growth rate, da/dN was found to be a random variable, approximately normally distributed with a mean value and standard deviation. The standard deviation was defined as

$$\sigma = \sqrt{\sum (X_i - \bar{X})^2/(n-1)}$$

where X_i is the value of da/dN per increment, $\bar{X}$ is the mean incremental crack growth rate and n is the number of overlapping incremental data points. From the same a and N data, sets of crack growth data were obtained over different averaging increments ΔC.

The crack growth rate data in all materials used in this study varied within the sample from increment to increment. They also varied with the width of the data averaging increment as expected. To evaluate this variation, a comparison of the standard deviations was made.

(a) *Effect of plate orientation*

Table 5, which is data selected from Table 4, shows a trend in standard deviation for the two basic notch orientations in the base plate. As expected, the crack grows slowly in the tougher transverse direction but, as not necessarily expected, the standard deviation is smaller.

Table 5. Effect of crack orientation (base plate/HY-80 crack growth data averaged over 0.51 mm increment obtained in air at 23°C, $\Delta K = 49.5\ \text{MPa}\sqrt{m}$, $R = 0.1$, 0.3 Hz, $n = 180$)

Base plate/HY-80 crack orientation	Specimen No.	Standard deviation (μm/cycle)	da/dN crack rate (μm/cycle)
T	13	0.013	0.541
	15	0.015	0.538
	6	0.012	0.537
	14	*0.015*	*0.538*
	Combined	0.014	0.538
L	4	0.016	0.660
	9	0.019	0.660
	10	*0.019*	*0.656*
	Combined	0.018	0.659
	$\sigma^2 = \frac{1}{K}(\Sigma\,\sigma_k^2)$		

(b) *Effect of crack increment*

If the data for all combinations of conditions in Table 4 is examined, as expected, the standard deviation decreases with increasing ΔC.

(c) *Effect of* ΔK

If the data in Table 6 is examined, it can be seen that, as expected, the mean rate increases with ΔK and the standard deviation on the same crack size increases as well. At much higher values of K, it would be expected that the standard deviation would decrease with increasing K as cracks do not deflect or meander at high ΔK as much as they do at lower values.

(d) *The effect of* R

The effect of R can easily be seen if the data subset in Table 7 is examined. The mean rates increase with R while standard deviation decreases.

(e) *The effect of weldment*

In the weldment containing specimens, the mean value is much slower than for the base plate and the ratio of standard deviation to mean rate is considerably greater (Table 8). This is because the cracks deviated from the plane during propagation considerably more than in the base plate specimens. Considering the microstructural heterogeneity of the material in the centre of weldment containing test specimens, it seem highly probable also that the crack growth and the variability of crack growth rate data would be affected by this as well. In effect, cracks crossing different weld zones halted and deflected more than the cracks propagating in base plate or single weld zones.

(f) *The effect of environment*

If the data in Table 9 is compared it can be seen that cracks grow faster in seawater than in air and that the standard deviation is larger in seawater. Cathodic current increases both the crack growth rate and standard deviation.

10. CONCLUSIONS

(1) The variability in crack growth rate data changes with material, orientation, environment, R and with ΔK.

(2) The crack growth in the weldments studied is slower than in the base plate giving a conservative operational overlap.

(3) A Monte Carlo technique for using the data presented in this report to acquire a statistical estimate of deviation from mean life in structural analysis is presented.

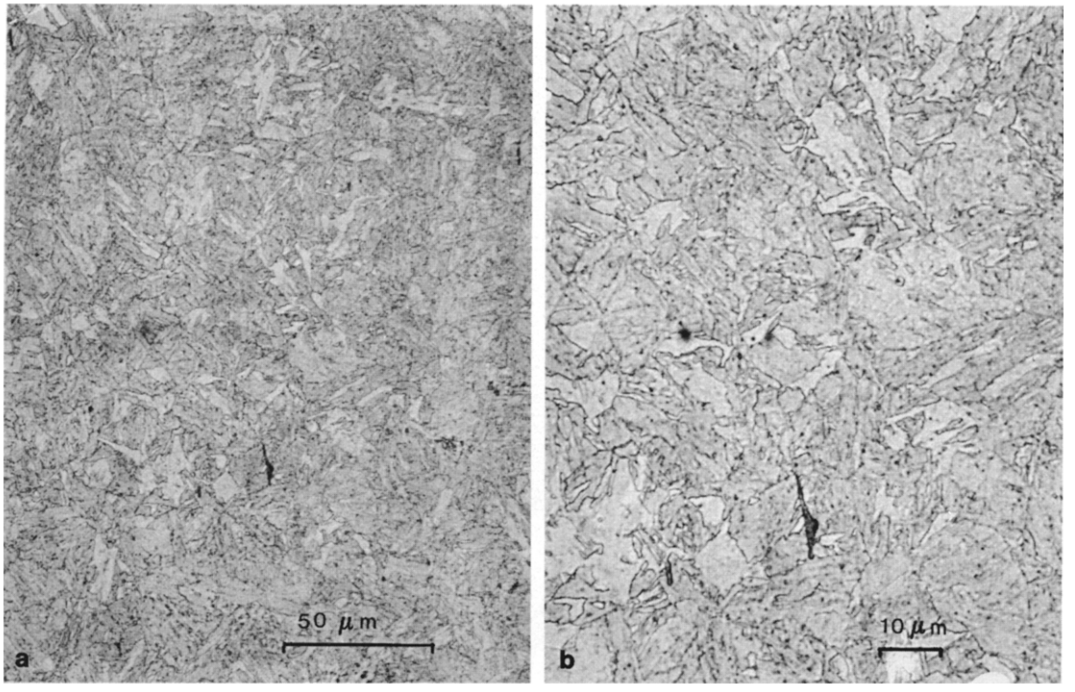

Fig. 11. General microstructure of base plate/HY-80.

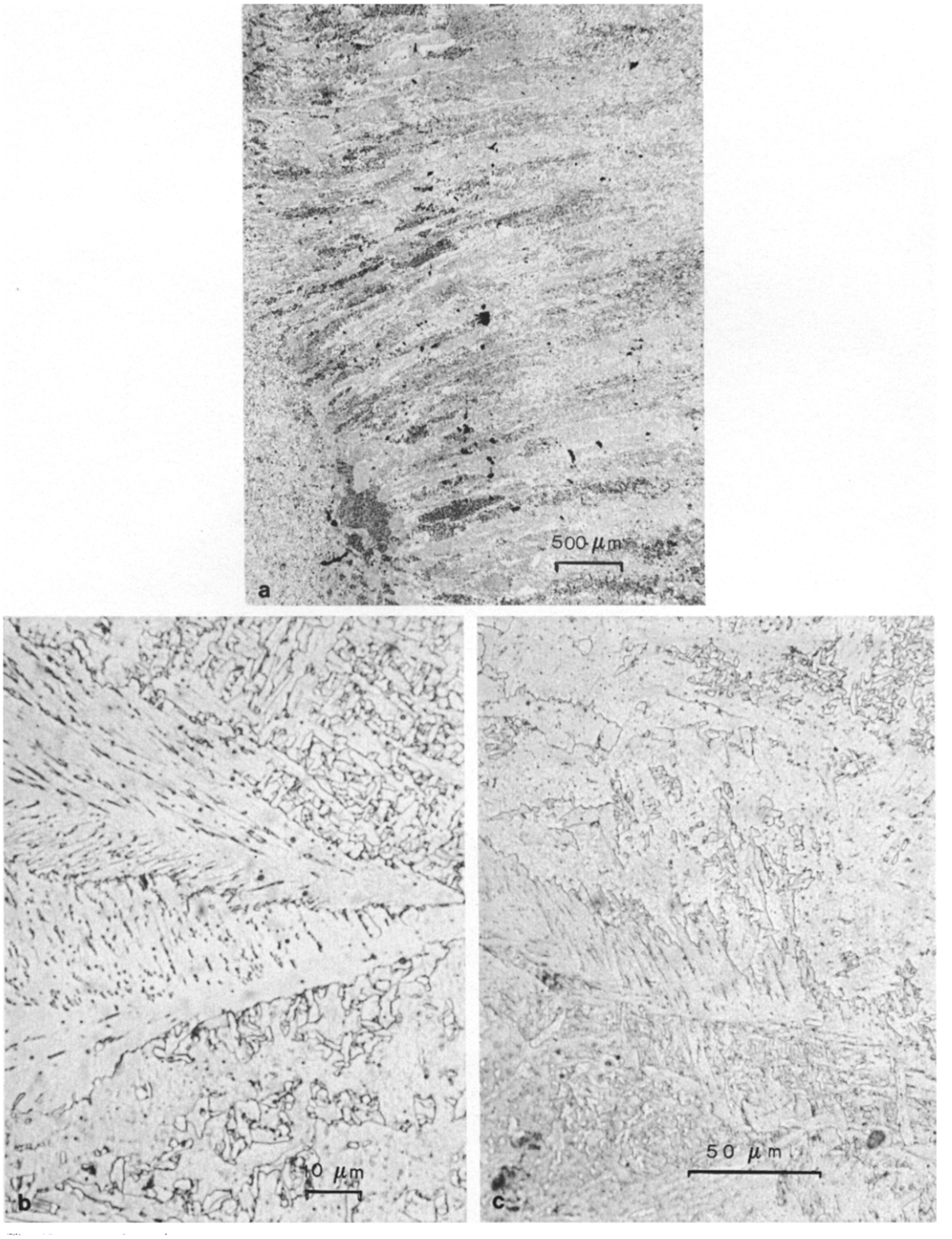

Fig. 12. Dendritic microstructure of 9/10 SMAW/E7018 weld.

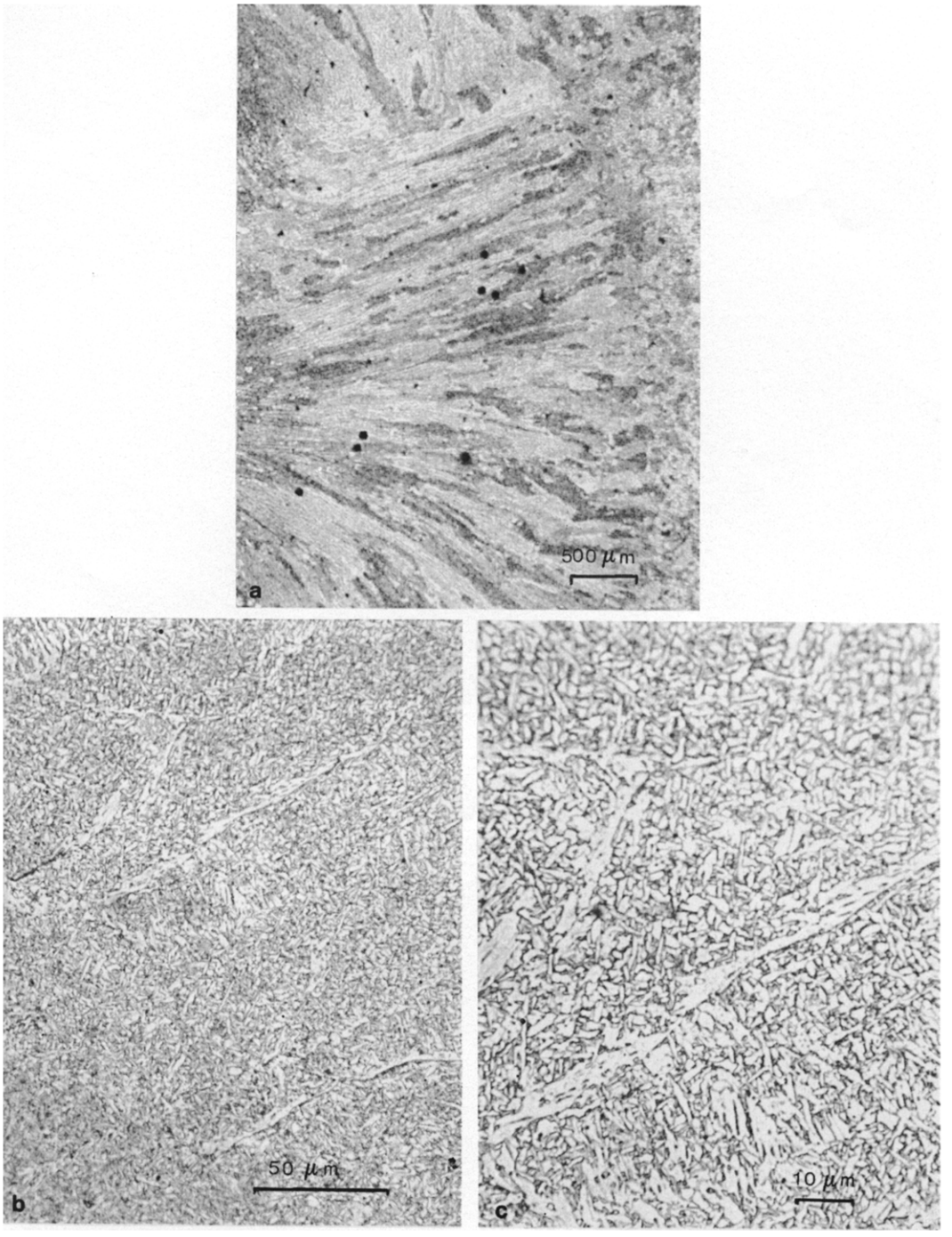

Fig. 13. Typical microstructure of 10 (266) MIG Espel flat weld.

Table 6. Effect of ΔK (base plate/HY-80 crack growth data averaged over 0.51 mm increment obtained in SW + CP at 23°C, $\Delta K = 49.5$ MPa $\sqrt{m}$, $R = 0.5$, 0.3 Hz, $n = 180$)

	ΔK	Mean da/dN (μm/cycle)	Standard deviation (μm/cycle)
90G1 (T)	22.0	0.168	0.007
	19.2	0.116	0.002
90G2 (T)	22.0	0.238	0.002
	24.7	0.281	0.003

Table 7. Effect of R (base plate/HY-80 crack growth data averaged over 0.51 mm increment obtained in SW + CP at 23°C, 0.3 Hz)

Specimen	ΔK, MPa$\sqrt{m}$	K_{max}, MPa$\sqrt{m}$	R	Incremental crack growth mean, da/dN μm/cycle	Standard deviation μm/cycle
T2	29.7	33	0.1	0.101	0.0146
TA6	16.5	33	0.5	0.186	0.0045
TA3	19.2	38.4	0.5	0.287	0.0034
C3	19.8	22	0.1	0.085	0.0105

Entire data sets used to calculate standard deviation.

Table 8. Effect of weldments (HY-80 weldments crack growth data averaged over 0.51 mm increment obtained in SW + CP at 23°C, $\Delta K = 22$ MPa$\sqrt{m}$, $R = 0.5$, 0.3 Hz, $n = 24$)

Plate	Specimen no.	Mean (μm/cycle)	Standard deviation (μm/cycle)
4 (260) MIG Generac Flat	4-5	0.085	0.011
4 (260) MIG Generac Flat	44-1	0.056	0.011
10 (266) MIG Espel Flat	10-3	0.088	0.022
10 (266) MIG Espel Flat	10-41	0.136	0.006
5/6 SMAW E11018M	5/6-22	0.120	0.022
7/8 SMAW E11018M	7/8-1	0.125	0.011
9/10 SMAW E7018	9/10-22	0.270	0.003
9/10 SMAW E7018	9/10-32	0.102	0.020
90E1 SMAW E9018M	90E1	0.194	0.036

Table 9. Effect of environment on standard deviation (HY-80 (T)t = 23°C, Hz = 0.3, $R = 0.1$)

Specimen	Test conditions ΔK, MPa$\sqrt{m}$	Environment	n	Incremental crack growth at 0.51 mm Mean μm/cycle	Standard deviation σ, μm/cycle
4A	19.8	Air	135	0.0226	0.0005
B3	19.8	SE	134	0.0489	0.0017
C2	19.8	SW + CP	118	0.0856	0.0061
T1	22	SW	149	0.0487	0.0100
T4A	22	SW + CP	76	0.0892	0.0202
T2	29.7	SW + CP	145	0.181	0.0147
T3	29.7	SW	49	0.206	0.0189

REFERENCES

[1] W. G. Clarke and S. Hudak, Jr, Variability in fatigue crack growth testing. *J. Test. Eval.* **3**, 454–476 (1975).
[2] D. F. Ostergaard, J. R. Thomas and B. M. Hillberry, Effect of Δa increment on calculating da/dN from a vs N data in *Fatigue Crack Growth Measurement and Data Analysis* (Edited by S. Hudak, Jr and R. J. Bucci), pp. 194–204 (1981).
[3] G. R. Yoder, L. A. Kooley and T. W. Crooker, Procedures for precision measurement of fatigue crack growth rate using crack-opening displacement technique, in *Fatigue Crack Growth Measurement and Data Analysis* (Edited by S. Hudak, Jr and R. J. Bucci), *ASTM STP*, 85–102 (1981).
[4] T. K. Betancourt and J. R. Matthews, Effects of the averaging increment ΔC on the scatter in da/dN data and mean life cycles in HY-80 steel plate. *J. Test. Eval. JTEVA* **15**, 20–29. (January 1987).
[5] J. F. Knott, *Fundamentals of Fracture Mechanics*. Butterworth, Toronto (1973).
[6] E. Roberts, Jr, Elastic crack edge displacement for the compact tension specimen. *Mater. Res. Stand.* **9**, 27 (1969).
[7] D. A. Jablonski and B. H. Lee, Automated fatigue crack growth rate testing using computer test system. Presented at SEECO '83, Digital Techniques in Fatigue, City University, London (28–30 March, 1983).
[8] A. Ditschun, Application of pulsed current techniques to welding HY-80 steel. DREA Contractor Report, DREA CR/85/421 (September 1985).
[9] M. Macecek and J. Belbeck, Research in narrow gap welding of HY-80 steels using the TIME process. DREA Contractor Report, DREA CR/86/434 (April 1986).

(*Received* 28 *November* 1988)